Smart Structures and Systems, *Vol. 24, No. 4 (2019) 491-506*
DOI: https://doi.org/10.12989/sss.2019.24.4.491

Earthquake effect on the concrete walls with shape memory alloy reinforcement

Hamid Beiraghi*

Department of Civil Engineering, Mahdishahr Branch, Islamic Azad University, Mahdishahr, Iran

(Received December 31, 2018, Revised July 31, 2019, Accepted August 3, 2019)

Abstract. Literature regarding concrete walls reinforced by super elastic shape memory alloy (SMA) bars is rather limited. The seismic behavior of a system concurrently including a distinct steel reinforced concrete (RC) wall, as well as another wall reinforced by super elastic SMA at the first story, and steel rebar at upper stories, would be an interesting matter. In this paper, the seismic response of such a COMBINED system is compared to a conventional system with steel RC concrete walls (STEEL-Rein.) and also to a wall system with SMA rebar at the first story and steel rebar at other stories (SMA-Rein.). Nonlinear time history analysis at maximum considered earthquake (MCE) and design bases earthquake (DBE) levels is conducted and the main responses like maximum inter-story drift ratio and residual inter-story drift ratio are investigated. Furthermore, incremental dynamic analysis is used to accomplish probabilistic seismic studies by creating fragility curves. Results demonstrated that the SMA-Rein. system, subjected to DBE and MCE ground motions, has almost zero and 0.27% residual maximum inter-story drifts, while the values for the COMBINED system are 0.25% and 0.51%. Furthermore, fragility curves show that using SMA rebar at the base of all walls causes a larger probability of exceedance 3% inter-story drift limit state compared to the COMBINED system. Static push over analysis demonstrated that the strength of the COMBINED model is almost 0.35% larger than that of the two other models, and its general post-yielding stiffness is also approximately twice the corresponding stiffness of the two other models.

Keywords: shape memory alloy; reinforced concrete wall; earthquake; drift

1. Introduction

Reinforced concrete (RC) walls in the structural industry have such advantages as high stiffness and strength (Beiraghi *et al.* 2016). From a seismic viewpoint, it is not economical to prevent the entire RC wall from extending the plasticity subjected to Design-Based Earthquake (DBE) or the Maximum Considered Earthquake (MCE). Design codes allow the occurrence of plasticity in some parts of a system during strong ground motions. Therefore, codes recommend reducing lateral loads when designing a system. In a slender cantilever RC wall, the occurrence of the flexural hinge is preferred to be located at the base region. Extension of one plastic hinge at the base of cantilever shear walls has been recommended by researchers and documents. (CSA Standard, 2005, NZS 3101, 2006, CEN EC8, 2004, Priestley *et al.* 2007, Paulay *et al*. 1992). In the philosophy of capacity design, the seismic design of structures is accomplished in such a way that during severe ground motion, the structure responds in a desirable and ductile manner. For cantilever RC walls, flexural yielding at the wall base is the primary mechanism for energy dissipation (Paulay *et al.* 1992). This approach has been recommended by the commentary of ACI318-14 (ACI 318, 2014). However, the dynamic response of slender cantilevered RC walls is mainly affected by higher-mode effects and researchers have demonstrated that greater than expected moment demand can develop at the mid-height of these walls due to the effect of higher mode of vibration (Eberhard *et al*. 1993, Panneton *et al*. 2005, Rutenberg *et al.* 2006, Ghorbanirenani *et al.* 2012, Luu *et al.* 2013, Beiraghi *et al*. 2018a-d).

Buildings designed in accordance with the modern structural codes are expected to undergo considerable structural and nonstructural damage during strong ground motion (Beiraghi *et al.* 2016). Normally, the design of structures is carried out for life-safety performance, in which the objective of design is to protect the lives of the occupants during a DBE event (FEMA 450). Damage to the RC wall may include steel reinforcement yielding or buckling, fracture of concrete and permanent horizontal drift after a severe event. Generally, damages in RC walls due to the plasticity extension are difficult to repair. Besides, buildings with large residual drifts require expensive structural repair and will often be out of service for long periods of time (Eguchi *et al.* 1998). If the residual drift is too severe, the structure may require demolition instead of repair.

However, RC walls have demonstrated reasonable performance under previous earthquakes (Fintel *et al.* 1995, Ghosh 1995). Chile earthquake in 2010 and New Zealand event in 2011 have demonstrated shortcomings that led to severe damage and collapse of mid-rise buildings (Saatcioglu *et al*. 2013, Wallace 2012, Elwood *et al.* 2013). For some buildings, damage of RC walls has caused

*Corresponding author, Mr.
E-mail: h.beiraghi@msh-iau.ac.ir

http://www.techno-press.com/journals/sss&subpage=7
ISSN: 1738-1584 (Print), 1738-1991 (Online)

permanent large drifts not economical to repair. It is believed that the design of a structure should comprise sustainable and resilient aspects that not only prevent brittle failure and loss of stability, but also incorporate a re-centering mechanism capable to recover the majority of the inelastic deformations. The re-centering concept, previously discussed by other researchers, can potentially reduce post-earthquake repair costs (Tremblay *et al*. 2008, Chancellor 2014).

Due to mentioned shortcomings, Shape Memory Alloys (SMAs) have attracted the interest of researchers, mainly because of their capability to recover lateral displacements upon removal of stress (super elastic SMA), or with the application of heat (shape memory effect). Furthermore, energy dissipation through hysteretic damping is another advantage of SMAs, as well as strength and displacement capacities, compared with conventional deformed reinforcement. Also, SMAs have such advantages as high fatigue and corrosion resistance. SMAs have a number of structural applications like reinforcement in new constructions, or as a new material to retrofit the existing structural elements (Alam *et al*. 2008, Song *et al*. 2006, Janke *et al.* 2005, Hamdaoui *et al*. 2019, Katariya *et al.* 2017).

Recently, in order to reduce the damage experienced during severe earthquakes, investigation of re-centering RC structural system behavior using SMA reinforcement has highly been emphasized. Super elastic SMAs have successfully been examined as internal reinforcement for new concrete constructions (Abdulridha and Palermo 2017, Cruz *et al.* 2013, Nakashoji *et al.* 2014, Nehdi *et al.* 2010, Saiidi and Wang 2006, Saiidi *et al.* 2009, Youssef *et al.* 2008). More recently, super elastic SMAs have also been investigated as external bracing systems to retrofit concrete structures (Cortés-Puentes *et al.* 2017).

In comparison with traditional steel reinforcement, the main deficiency of SMAs is their higher cost. Thus, researchers tend to optimize their application. Furthermore, lower elastic modulus (approximately 60 GPa) compared to conventional steel reinforcement (200 GPa) may lead to larger displacements of structures or elements subjected to service loads.

Some researchers have investigated the behavior of RC elements with SMA rebar and demonstrated the capability of SMAs to restore a RC member to its original position (Cortés-Puentes *et al*. 2018). Besides, experimental and numerical studies demonstrated that super elastic SMAs reduce residual deformations and provide excellent energy dissipation in RC walls (Abdulridha and Palermo 2017, Ghassemieh *et al.* 2012).

Generally, the flag-shaped hysteresis of SMA rebar is appealing to earthquake engineering researchers, as it can reduce residual deformations subjected to earthquake loads. At low strain (<1%), the rather large modulus of elasticity of the austenite phase can limit deformation exerted by service loads. The intermediate strain plateau (between 1% to 6%) with low modulus of elasticity, can limit the force transmitted to adjacent structural components when subjected to relatively large displacements. (McCormick *et al.* 2007).

Saiidi and Wang (2006) and Saiidi *et al*. (2009) also accomplished shake table and quasi-static tests on concrete bridge columns, reinforced by SMA longitudinal reinforcement in plastic hinge area. Reported results indicated that SMA-reinforced columns significantly reduced residual deformation.

Alam *et al.* (2009) investigated the seismic response of concrete frames reinforced by SMAs subjected to strong earthquakes through non-linear time-history analyses. Results show that SMA RC frames could restore most of their large inelastic deformation even after a strong earthquake.

However, previous evaluations were mainly focused on super elastic SMA rebar in RC beam, column, and beam–column joints, and to the knowledge of the author, literature regarding RC walls reinforced by super elastic SMA bars are still seldom. In addition, the seismic behavior of a system concurrently including distinct steel reinforced RC wall, as well as super elastic SMA reinforced wall, has not been studied enough. In this paper, the seismic response of such a system is compared to both conventional steel RC concrete wall, and wall with SMA rebar only at the first story. Nonlinear time history analysis (NLTHA) at MCE and DBE levels is conducted and the main responses like IDR and residual IDR are investigated. Furthermore, Incremental dynamic analysis (IDA) procedure is used to accomplish probabilistic seismic studies by creating fragility curves.

2. Model introduction and design

The floor plan of the assumed 6-story building is depicted in Figure 1. For seismic design, the proposed buildings are loaded and analyzed solely along x direction. RC walls are regarded as the mere lateral load resisting systems in the examined structures and the connections between floor beams and the columns are of a pin type. The dead and live loads of the floors are 550 and 200 Kgf/m2, respectively. For each selected building, there are four RC walls along x direction which resist all the lateral loads. Three different approaches are investigated in this paper. In the first one, denominated as STEEL-Rein., all the walls are conventional RC walls with steel reinforcement. In the second named as SMA-Rein., only SMA rebar is used at the first story of all the walls and conventional steel rebar is used for wall reinforcement at other stories. In the third approach known as COMBINED model, two of the four walls are conventional steel RC walls, and the two remaining walls have SMA rebar at the first story and steel rebar at upper stories. In practice, special couplers are used to connect steel bars to SMA bars. In the designed numerical model, only RC walls are modeled as a two dimensional steel RC walls. Of course, the proper amount of gravity load carried by the RC wall is applied in the numerical model at floor levels, and also the corresponding mass coefficient is supposed to apply at each story of the hypothetical building. Each story has a height of three and a half meters, and the connection of the wall to the base is a fixed type. The ETABS software was used to create elastic

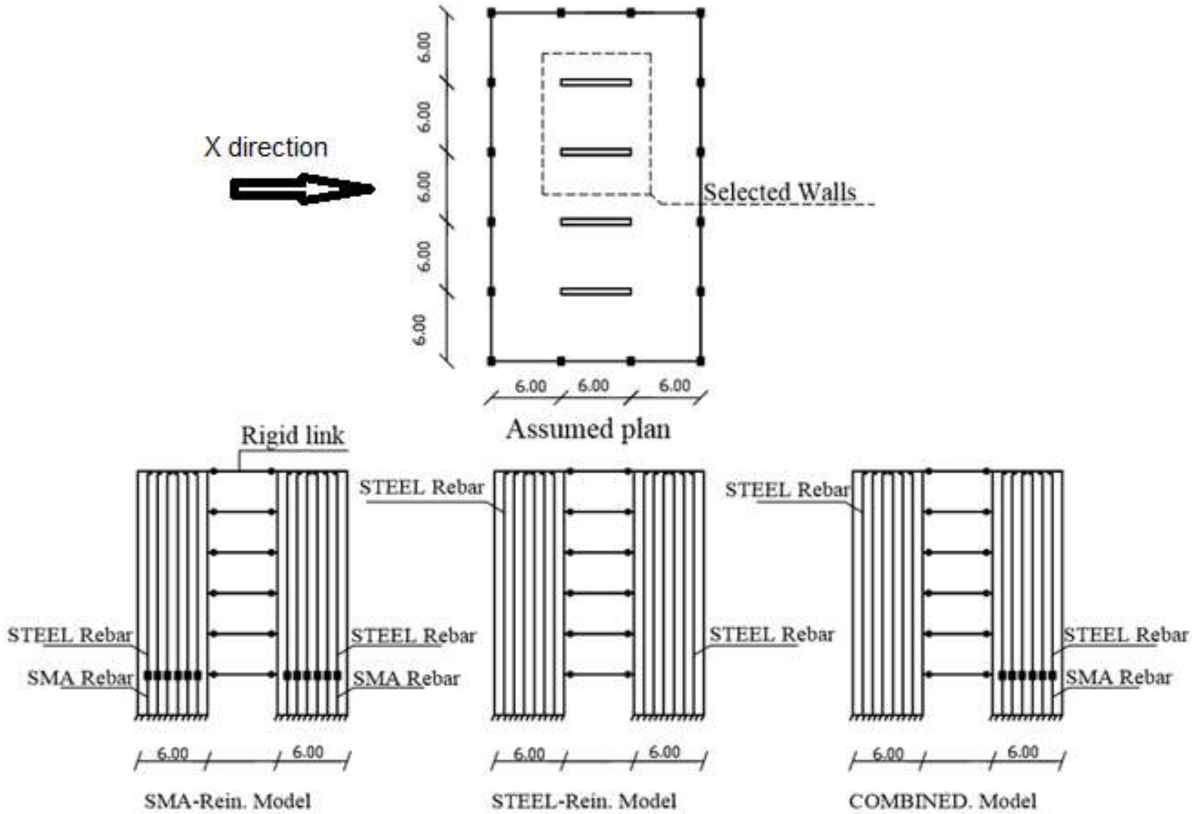

Fig. 1 Floor plan of the assumed 6-story building and selected two dimensional idea for SMA-Rein., STEEL-Rein. and COMBINED models (dimensions are in meter)

numerical models and analyze the two dimensional RC walls (ETABS, Version 13.1.1, 2013). Shell element was used to model RC walls.

RC walls were designed based on the ASCE-7 and ACI318-14 (ACI 318, 2014; ASCE/SEI 7-2010). The proposed nominal compression strength of concrete in the RC wall was 45MPa and the nominal yielding strength of the steel rebar was 400MPa. To take into account the concrete cracking on lateral stiffness of the examined RC wall, flexural stiffness was reduced by multiplying a factor equal to 0.5. This coefficient was applied so that the moment of inertia of the wall's gross cross-section decreased. This was in accordance with the recommendation of ACI 318-14 (Sections 8.8 and 10.10).

The main characteristics of the designed RC walls are represented in Table 1. The thickness of RC wall was invariable along the height. The vertical reinforcement ratio of each story is different, and the last two stories require minimum reinforcement ratio. The distribution of longitudinal rebar was uniform within each cross-section. The amount of vertical reinforcement was calculated in such a way that the nominal flexural strength in each section was greater than the design envelope.

The natural free vibration periods, mode shapes and modal mass participation factors were obtained using modal analysis and response spectrum analysis (RSA) procedure. More than 96% of the modal participation mass ratio belongs to the first three translational modes of vibration along the X direction. A 5% damped DBE elastic response spectrum was used for the design procedure (see Fig. 2). To obtain the elastic design demand, a reduction factor named response modification factor, R, equal to 5, was used to reduce elastic response demands (ASCE/SEI 7-2010).

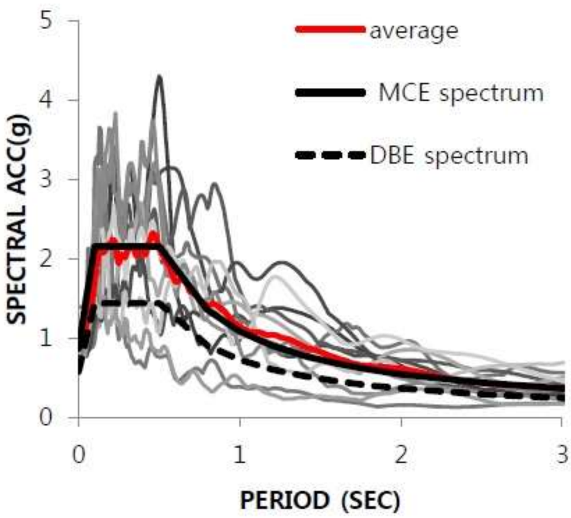

Fig. 2 Elastic response spectrum for DBE, MCE and 5% damped individual records.

Table 1 The main characteristics of the designed RC wall systems

ITEM		
Total height (m)		21
Total seismic weight (tonf)		1170
Wall length, Lw (m)		6
Wall thickness (m)		0.3
$P/(A_g.f_c)$		0.089
Boundary zone (No. of stories)		ST1 to ST3
Modified base shear from RSA used for design (tonf)		207.8
Base shear via the equivalent static method, V (tonf)		244
Period of free vibration (s)	T1	0.744
	T2	0.139
	T3	0.061
Modal P.M.R	Mode 1	0.68
	Mode 2	0.22
	Mode 3	0.064
	Mode 4	0.023

Table 2 The wall vertical reinforcement ratio

Story no.	**ρ**
1	1.22%
2	0.85%
3	0.52%
4	0.32%
5	0.25%
6	0.25%

Besides, the base shear force obtained from RSA was modified so that its quantity was equal to 0.85 times the base shear demand calculated from the equivalent static method, V. ASCE 7 states that when the combined base shear demand obtained from RSA reduced by R factor (denominated as V_t) is less than 85% of the base shear via equivalent static method (V), the forces are multiplied by 0.85 V/V_t (ASCE/SEI 7-2010). Since this condition controlled the design, effective response modification factor, Reff, is less than 5 (Table 1). The wall vertical reinforcement ratio is shown in Table 2.

3. Nonlinear specifications

Comparing the cyclic responses of numerical fiber model of slender RC walls subjected to lateral loads, with corresponding responses of large-scale experimental laboratory test, demonstrated acceptable conformity (Orakcal *et al.* 2006). Fiber models are widely recognized to simulate the seismic behavior of RC walls. Neutral axis movement in a cross-section of a RC wall subjected to cyclic or seismic loading, can be predicted by fiber element modelling, which has preference over lumped-plasticity models (ATC-72, 2010). NLTHA of the prototype models was implemented using a fiber element for the RC wall in Seismostruct (2018) software.

A uniaxial stress-strain relationship for steel model proposed by Menegotto and Pinto (1973) was used for steel rebar. Also, a uniaxial model for super elastic shape-memory alloys (SMAs), proposed by Auricchio and Sacco (1997) was adopted. This model includes a constant stiffness for both the fully austenitic and fully martensitic behavior, and is also rate-independent. This is a uniaxial nonlinear constant confinement model, initially programmed by Madas (1993), which follows the constitutive relationship proposed by Mander *et al.* (1988) and the cyclic rules proposed by Martinez-Rueda and Elnashai (1997). The confinement effects provided by the lateral transverse reinforcement are incorporated through the rules proposed by Mander *et al.* (1988), whereby constant confining pressure is assumed throughout the entire stress-strain range. The confined concrete stress–strain relation was applied by using a modified Mander model (Mander *et al*. 1988). Expected compressive and tensile strength of concrete were 58 and 2.2 MPa in the numerical model, and the confinement effect was applied in this model. The strain-stress relationship for the mentioned material has been plotted in Figure 3.

3.1 RC wall verification

Experimental work on a slender RC wall subjected to cyclic lateral loading was used to assess the accuracy of the modeling in the software SEISMOSTRUCT (2018). Capacity design has been used to design this specimen to conduct flexural hinge formation at its base (Orakcal and Wallace 2006). A constant axial force of 0.07Agfc, where Ag is the area of the wall cross section and fc is the concrete compression strength, was implemented and cyclic lateral displacement was exerted at the top of the wall. Fig. 4 compares the hysteresis loops resulted from numerical and experimental works. The horizontal axis is the lateral displacement at the top of the specimen. The overall resulted curves from the numerical model and experimental work are roughly similar and demonstrate the software capability.

3.2 Ground motion selection

Selection of ground motion records was important to accomplish NLTHA and IDA. To evaluate the response of the systems subjected to DBE and MCE level events, the records should be scaled appropriately. The 5% damped response spectrum curve of the MCE level was 1.5-times the one of DBE level (ASCE/SEI 7-2010). From the FEMA P695, a total set of 16 horizontal far-fault records was selected from the strong ground motions set (2009). All selected records were fault normal components of the strong ground motions, and their records were obtained from the PEER NGA data base. The specification of accelerograms are represented in Table 3 and their spectra are plotted in

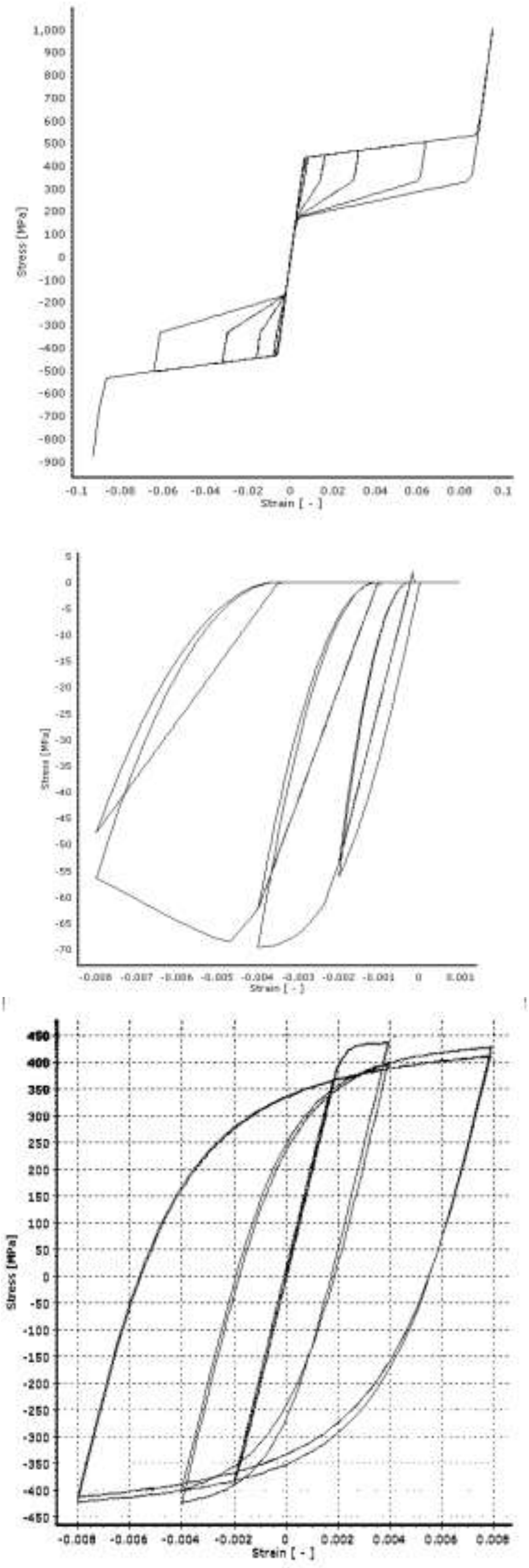

Fig. 3 The strain-stress relationship for the SMA, concrete and steel bar material

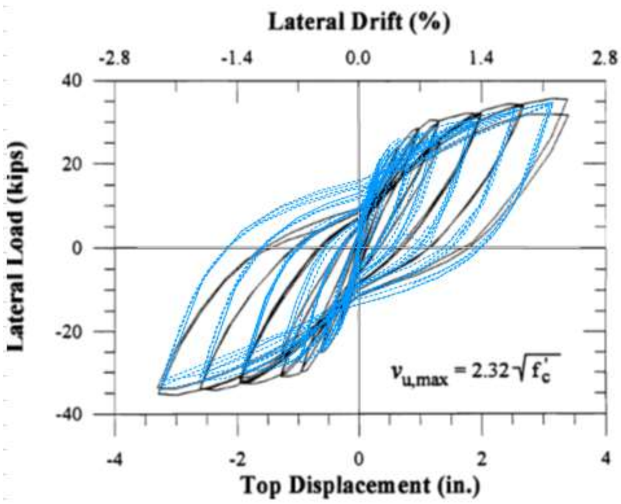

Fig. 4 Comparing the hysteresis loops resulted from numerical (blue curve) and experimental (black curve from Orakcal and Wallace, 2006) works

Fig. 2. The record intensity was scaled as recommended by the ASCE7. The ground motions were scaled in such a way that the average of the 5% damped spectrum graph, for periods ranging from 0.2T to 1.5T, located above the assumed target spectrum. T is the fundamental period of the natural free vibration of the elastic structure (ASCE/SEI 7-2010). The scaled spectra for the individual selected records and their average are shown in Fig. 2.

3. Results from NLTHA

Fig. 5 shows the average maximum IDR demand envelope of the SMA-Rein., COMBINED and STEEL-Rein. models along the height of the structure are subjected to the DBE level record set. The horizontal axis represents the values of the maximum IDR and the vertical axis represents the normalized height. The maximum permissible IDR at the level of the DBE events is 2% in accordance with the ASCE/SEI 7-2010 code. It is observed that the maximum IDR demand occurs in the STEEL-Rein model at the last floor and is about 1.6%, while this value for the COMBINED model and the SMA-Rein. model is 1.49% and 1.4% respectively, all of which are below the permissible limit.

Also, the maximum residual IDR demand of each models subjected to the effect of each record in the form of a bar chart at DBE level is shown in Fig. 6. According to experts, if the amount of residual IDR in a structure exceeds 0.5% under the influence of an earthquake, demolition of the building for renovation is almost inevitable (McCormick *et al.* 2008). The maximum residual IDR demands of the SMA-Rein., COMBINED and STEEL-Rein models under the influence of DBE level earthquakes are 0.05%, 0.13% and 0.18%, all of which are less than 0.5%. It is obvious that the maximum residual IDR in the SMA-Rein. model is significantly lower than its corresponding value in the other two structures.

Table 3 Ground motion specifications selected for NLTHA and IDA

	Event name	Year	Station	Record duration(s)	PGA* (g)	PGV** (m/s)	M	Site-to-source distance (km)
1	Kocaeli, Turkey	1999	Arcelik	30	0.22	40	7.5	53.7
2	Superstition Hills	1987	Poe Road (temp)	22.3	0.45	36	6.5	11.2
3	Landers	1992	Yermo Fire Station	44	0.24	52	7.3	86
4	Superstition Hills	1987	El Centro lmp. Co.	40	0.36	46	6.5	35.8
5	Imperial valley	1979	El centro Array#11	39	0.38	42	6.5	29.4
6	Chi chi, Taiwan	1999	Chy101	90	0.44	115	7.6	32
7	Imperial valley	1979	Delta	100	0.35	33	6.5	33.7
8	San Fernando	1971	LA-Hollywood Stor	28	0.21	19	6.6	39.5
9	Kobe, Japan	1995	Shin- Osaka	41	0.24	38	6.9	46
10	Kocaeli, Turkey	1999	Duzce	27.2	0.36	59	7.5	98.2
11	Duzce	1999	Bolu	56	0.82	0.62	7.1	41.3
12	Northridge	1994	Canyon Country-WLC	20	0.48	45	6.7	26.5
13	Loma Prieta	1989	Gilroy Array	40	0.56	45	6.9	31.4
14	Hector Mine	1999	Hector	45.3	0.34	42	7.1	26.5
15	Chi-Chi, Taiwan	1999	TCU045	90	0.51	39	7.6	77.5
16	Northridge	1994	Beverly Hills - Mulhol	20	0.52	63	6.7	13.3

* PGA: Peak ground acceleration; ** PGV: Peak ground velocity.

For earthquake No. 3 at the DBE level, the time history of the axial strain demand for the longitudinal rebar at two ends of the wall at first story are shown in Fig. 7. It is observed that in the conventional RC wall (STEEL-Rein. model), the residual strain demand at the end of the strong motion in one rebar is about 0.7%, while this value is approximately zero in the SMA-Rein. model. This quantity is about 0.4% for the corresponding steel rebar of COMBINED model and almost zero for SMA rebar of this model.

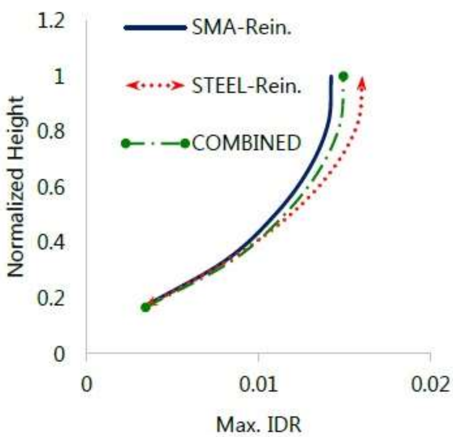

Fig. 5 Average maximum IDR demand envelope of the SMA-Rein., COMBINED and STEEL-Rein. models along the height of the structure subjected to the DBE level records

Also, Fig. 8 represents the time history of curvature ductility demand for the wall of each story under earthquake No. 3 at the DBE level. Curvature ductility values are obtained by dividing the curvature demand of a wall by the yielding curvature. For this purpose, the proposed Paulay *et al.* (1992) relationship is used to calculate the curvature ductility as follows

$$\emptyset_y = \frac{1.8\varepsilon_{ye}}{l_w} \tag{1}$$

In the above equation, $\emptyset_y$ is the yielding curvature of the reinforced concrete wall, ε_{ye} is the expected yielding strain of the reinforcement, and l_w is the length of the wall. The curvature ductility demand can be calculated from the following equation

$$\mu_\emptyset = \frac{\emptyset}{\emptyset_y} \tag{2}$$

Fig. 8 shows that in SMA-Rein. and COMBINED models, the maximum curvature ductility demand, subjected to the selected earthquake at the DBE level occurs at the first story, with a value of about 4 and 3.3, respectively, while the maximum curvature of the STEEL-Rein. model occurs in the fourth story, and its value is about 4.6. It is worth noting that the maximum curvature ductility of the STEEL-Rein. model at the first story is about 2.3, which is half the corresponding value of the fourth story. The fact that the curvature demand in the middle of a slender wall, with conventional steel rebar under severe earthquake, can be higher than the corresponding values at the base level, has already been expressed by experts (Eberhard *et al*. 1993, Panneton *et al*. 2005, Rutenberg *et al*.

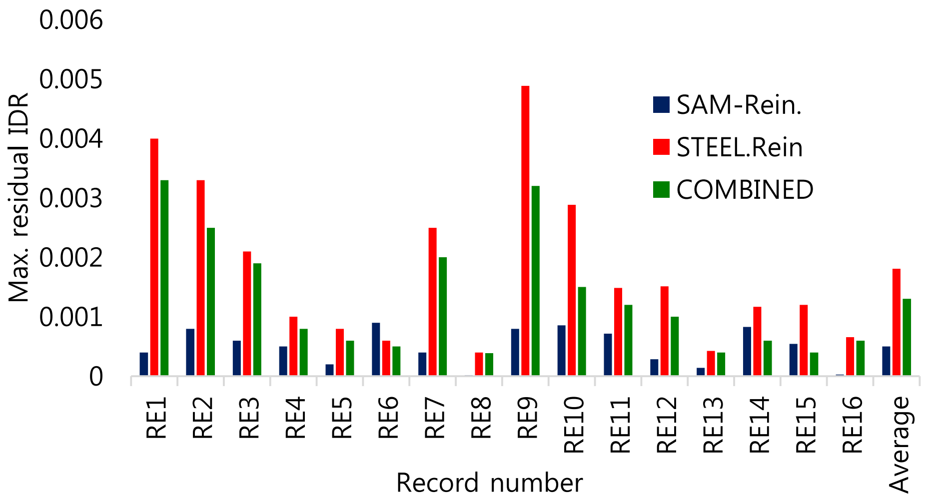

Fig. 6 Maximum residual IDR demand of each models subjected to the effect of each record in the form of a bar chart at DBE level

2006, Ghorbanirenani *et al.* 2012, Luu *et al*. 2013). The presence of SMA rebar at the first story of the SMA-Rein. and COMBINED models tends to concentrate the curvature plasticity demand at this story, and to reduce the intensity of plasticity development in higher regions. This will control the damage at the mid-height of the RC walls, because the mid-height of the walls often lacks the specific characteristics for concrete confinement and boundary elements. The occurrence of plasticity at mid-height can lead to widespread and undesirable failures.

The mean maximum IDR demand envelope along the height of the RC walls subjected to the earthquakes at MCE level intensity are shown in Fig. 9. It is observed that in the SMA-Rein. model, the mean maximum IDR demand occurs at the last story and is almost 4.6%. This quantity is approximately twice the corresponding value in the STEEL-Rein. structure. The maximum IDR for the COMBINED model is also at the 6TH story, and is about 2.8%. The LATBSDC (Los Angeles Tall Buildings Structural Design Council) guideline requires that the average maximum IDR demand at MCE level event is less than 3%, so the SMA-Rein. model is far beyond the stated value. Therefore, the use of SMA rebar in the first story of all walls of a structure is not recommended. On the other hand, for the models of this research, if SMA rebar is used in 50% of the walls at the first story, and traditional steel rebar is used in other stories as well as in other walls, the maximum IDR will be less than the permissible limit of 3%.

The bar chart for maximum residual IDR demand of each earthquake at the MCE level is presented in Fig. 10. It is observed that in the model with SMA rebar in all walls of the first story (SMA-Rein. model), the average maximum IDR demand is about 0.25%.

For the conventional RC wall, this quantity is about 1.27%, whereas, for COMBINED model, where only half of the walls at the first story includes SMA rebar, it is about 0.51%.

Fig. 7: Time history of the axial strain demand for the longitudinal rebar at two ends of the wall at first story for earthquake No. 3 at the DBE level (bar1 and bar2 correspond to the longitudinal rebar at two ends of the wall).

Hysteretic curves for the first floor wall subjected to earthquake No. 3 at the MCE level are plotted in Fig. 11. The horizontal axis is the first story displacement relative to the base, and the vertical axis is base shear pertaining to one wall. Minimum displacement belongs to STEEL-Rein. model, while maximum displacement belongs to SMA-Rein. model. The maximum base shear demand is much larger than the design base shear force. The reason is the effect of higher modes of vibration as well as over-strength.

Fig. 12 compares the push over results for the studied systems subjected to a triangular load pattern. Horizontal and vertical axes are maximum roof drift and base shear demand, respectively. The general trend of the responses for STEEL-Rein. and SMA-Rein. models are similar. However, the yielding of the SMA-Rein. model occurs at the lower base shear, and its general post-yielding stiffness is also lower. The strength of the COMBINED model is almost 0.35% larger than that of the two other models, and its general post-yielding stiffness is also approximately twice the corresponding stiffness of the two other models. It seems that the reason for this result is that in the COMBINED model subjected to lateral push over force, plasticity does not concentrate at the base. The base shear strength for the STEEL-Rein. model is almost 1.25 times the design base shear that is because of over-strength effect.

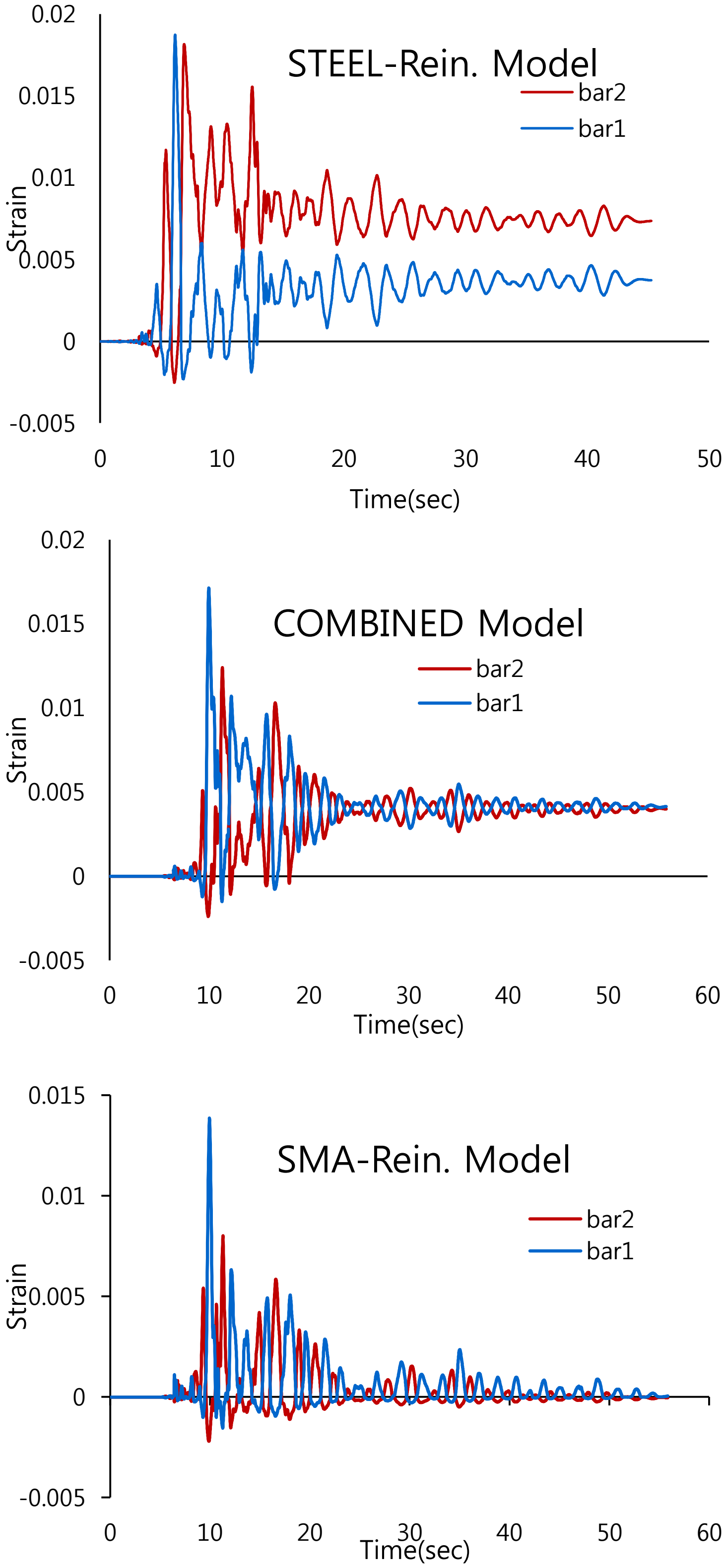

Fig. 7 Time history of the axial strain demand for the longitudinal rebar at two ends of the wall at first story for earthquake No. 3 at the DBE level (bar1 and bar2 correspond to the longitudinal rebar at two ends of the wall)

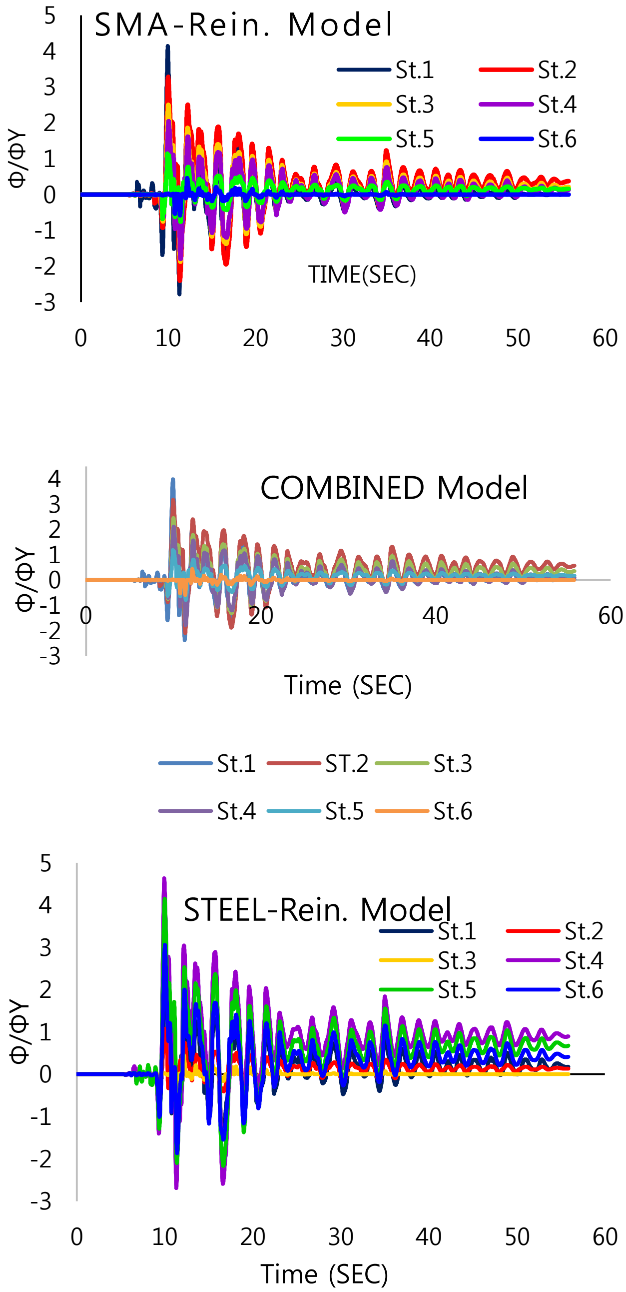

Fig. 8 Time history of curvature ductility demand for the wall of each story under the earthquake No. 3 at the DBE level

4. Results from IDA

Incremental Dynamic Analysis (IDA) is a parametric study process that rigorously investigates system performance subjected to seismic loads. In an IDA analysis, a structure is subjected to a set of ground motion records of increasing intensity. Using IDA procedure has been extended growingly and is considered as a valuable method for the performance assessment of buildings subjected to earthquakes (Vamvatsikos *et al.* 2002). To apply an IDA for a specified earthquake record, the time history is scaled to different levels of intensity by multiplying different coefficients. At first, the coefficient is so small that the system remains in linear range and increases gradually until either structural instability occurs, or the obtained inter-story drift demand becomes extremely large. Finally, a number of graphs named IDA, depicts the selected responses versus the accelerogram intensity levels. Commonly, a large number of non-linear dynamic analyses are required to obtain IDA curves as explained comprehensively by Vamvatsikos and Cornell (Vamvatsikos *et al.* 2002). IDA is a useful procedure to evaluate building performance, adopted in the latest FEMA documents such as FEMA P-58 (FEMA P-58, 2012), FEMA P-695 (FEMA P-695, 2009), etc.

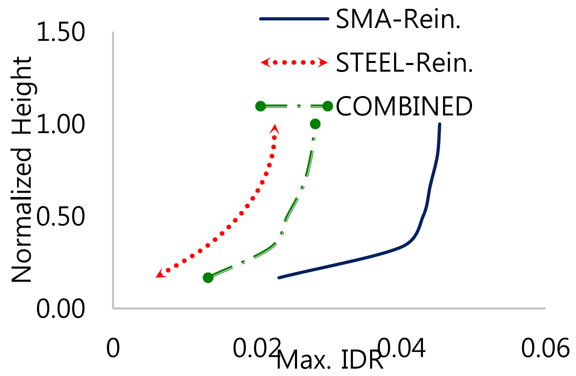

Fig. 9 Mean maximum IDR demand envelope along the height of the RC walls subjected to the earthquakes at MCE level intensity

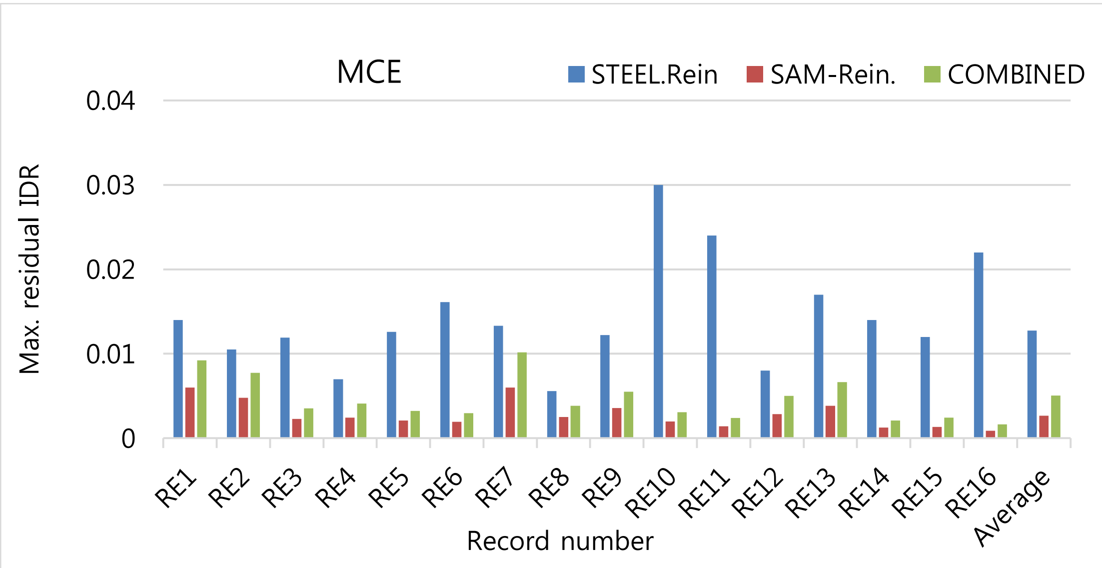

Fig. 10 Bar chart for maximum residual IDR demand of each earthquake at MCE level

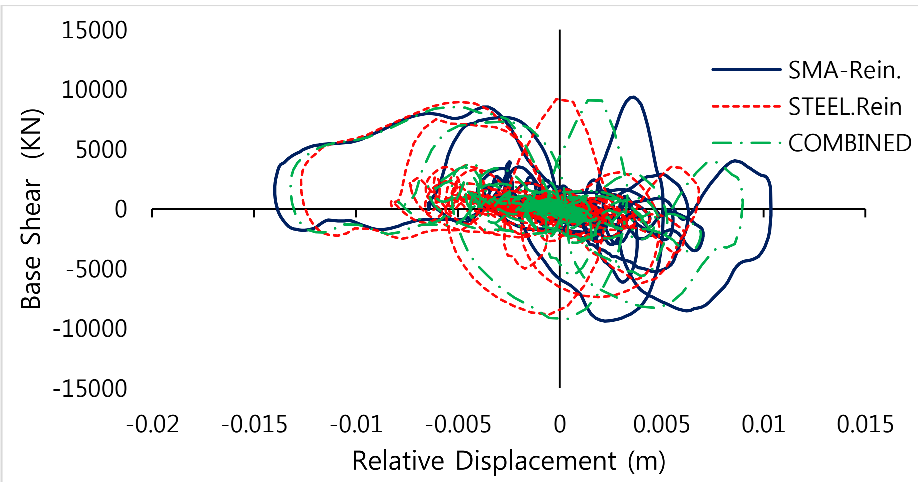

Fig. 11 Hysteretic curves for the first floor wall subjected to earthquake No. 3 at the MCE level

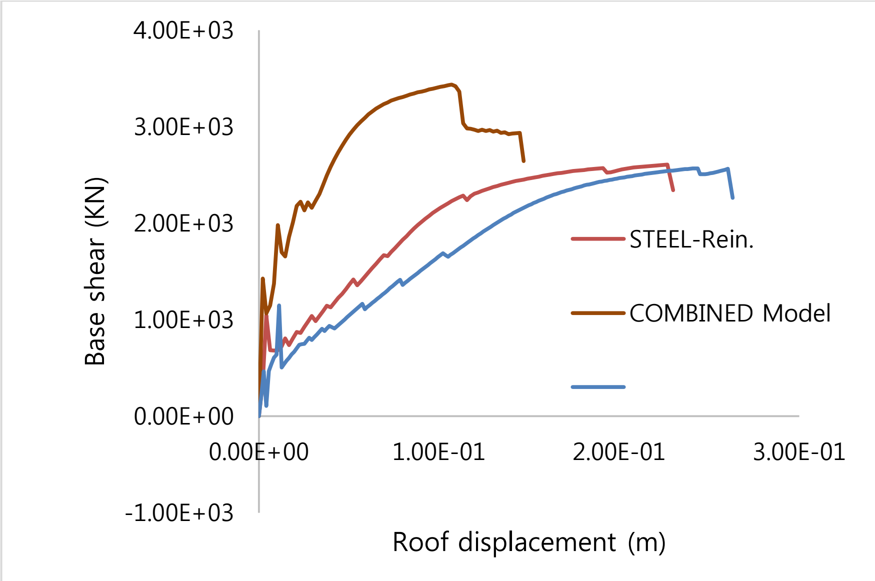

Fig. 12 Comparing push over results for the studied systems subjected to a triangular load pattern

As mentioned earlier, seismic response of a structure in IDA process is commonly represented through the relationship between Damage Measure (DM) of a system and Intensity Measure (IM) parameter of the ground motion record. Selection of DM and IM depends on the purpose of the research and requires careful definitions. IMs of ground motion records can be considered by a variety of parameters like PGA, PGV or 5% damped first-mode spectral acceleration Sa (T1,5%), etc. For no near-fault records, Sa (T1,5%), as well as PGA, are suitable and effective IMs and researchers have utilized both parameters in their investigation (Sadraddin *et al.* 2016). Furthermore, compared with PGA, Sa (T1,5%) yields more consistent outcomes, as discussed by a number of researches (e.g. Dhakal et al., 2006; Vamvatsikos and Fragiadakis 2010). Besides, the latest FEMA documents also use Sa (T1,5%) to carry out IDA for developing fragility functions (FEMA P-58, 2012; FEMA P-695, 2009 372). Therefore, in the current study, Sa (T1,5%) was adopted as the IM.

4.1 Performance measure

Lateral story displacement and inter-story drift are regarded as the most recognized DMs in seismic analysis of structures (Kruep 2007). Acceleration of floors is also a useful response for non-structural damage evaluation, while maximum inter-story drift is a proper choice for the assessment of structural damage (FEMA P-58, 2012). This research focuses on the structural evaluation of RC walls with different SMA arrangements. The maximum inter-story drift ratio was then designated as the DM.

A performance measure is a way to assess the results associated with the response of a building subjected to strong events, in such a way that are meaningful to decision-makers. Documents and researchers have used a variety of performance measures. In order to recognize the expected performance of a building subjected to earthquakes, standards have commonly used a series of well-known standard performance levels, such as Operational, Immediate Occupancy, Life Safety, and Collapse Prevention. These performance limit states are described by ranges for allowable strength and deformation demands on structural and nonstructural elements. For instance, the explanation for Slight, Moderate, Extensive, and Complete structural damage states for a variety of structures has been described by the HAZUS MR4's (National Institute of Building Sciences, 2004). Descriptions of that document are qualitative and generally useful for experimental works. For analytical models, fragility curves are developed based on numerical models and direct observation of mentioned states is almost impossible. The inter-story drift ratio is a well-known DM in the numerical analysis that can describe the limit state or performance level. Performance limit states for RC walls were adopted based on inter-story drift from previous standards/recommendations. The values are 0.5%, 1% and 2% for IO, LS and CP performance levels of RC walls (ASCE 41-13, FEMA 356, ACI 374.2R-13). It is worth noting that there is not an agreement about the CP performance level. One recognized concept is that CP performance limit state depends on the onset of strength deterioration, and this opinion depends on the ductility capacity of structural elements. In this study, the utilized limit states are also adopted from FEMA 356.

Besides, according to LATBSDC, for collapse prevention evaluation, the average of absolute values of the maximum inter-story drift ratios from a suite of analyses shall not exceed 3%. Therefore, this limit state is also studied in the present research. An inter-story drift limit of 0.03 has been judged suitable by experts in recent documents for the collapse prevention level. In general, it is believed that up to this story drift, systems with proper yielding mechanisms and appropriate detailing will perform well (without significant strength loss), and that nonstructural components will not cause a major life safety

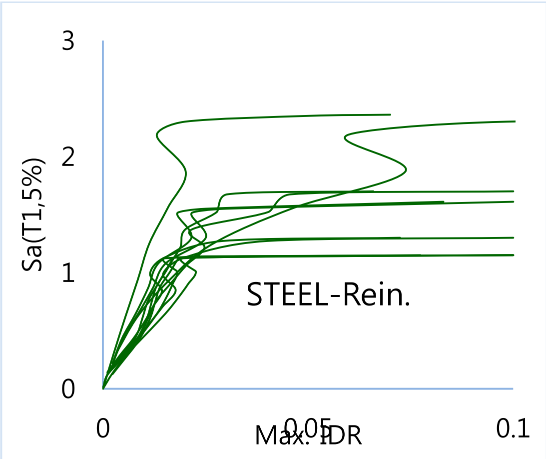

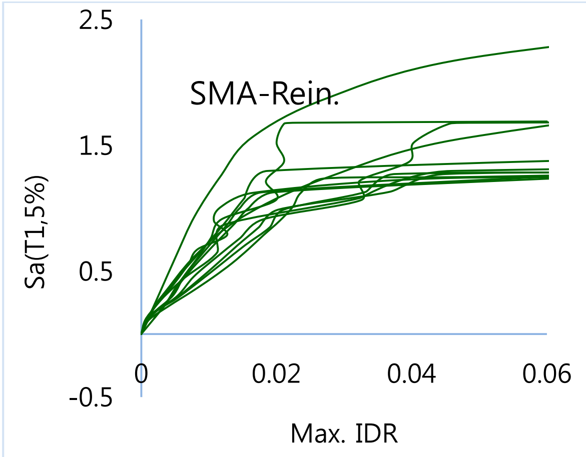

Fig. 13 IDA curves for SMA-Rein. and STEEL-Rein. models

hazard (LATBSDC 2.11).

Eventually, IDA process was accomplished on the examined numerical models along x-directions. The IDA curves are plotted in Fig. 13 for SMA-Rein. and STEEL-Rein. models. These IDA curves were created via a series of nonlinear time history analyses when each selected record was applied to the RC wall models with increasing intensity. The smallest scale factor quantity was applied in such a way that, the PGA of the record scaled to 0.1 g and gradually increased by a 0.1g step until RC wall models collapsed or underwent large IDR.

4.2. Fragility analysis results and discussion

IDA curves can help to evaluate the seismic vulnerability of the examined RC walls, by preparing fragility curves for a system at each limit state. Fragility curves graphically demonstrate the probability of exceeding a specified limit state at a selected intensity of earthquake excitation, represented as

$$f_{DL} = P(DL|IM) \tag{3}$$

Where, IM is the selected ground motion intensity measure and DL is the performance limit state. P is the probability of exceeding a specified limit state. In this research, data points IM=x (i.e., Sa (T1, 5%) pertaining to the 16 IDA curves corresponding to each determined limit state were assumed to be log-normally distributed (i.e., Ln(x) is normally distributed). Therefore, the probability of exceeding a damage level (DL) can be determined as

$$P(\leq DL) = \Phi\left(\frac{Ln(x) - \theta}{\beta}\right) \tag{4}$$

where $P(\leq DL)$ is the probability that a ground motion with IM = x will cause the system to exceed the specified limit state. Φ is the standard normal cumulative distribution function. θ and β are the mean and the standard deviation of Ln(x), sometimes known as the dispersion of IM, respectively. Eq. (1) demonstrates that the IM values of an earthquake set corresponding to a given limit state for a structure are log normally distributed, and this is a recognized assumption confirmed by a number of researchers (e.g., Ibarra and Krawinkler 2005, Porter *et al.* 2007, Bradley 2013, Eads *et al.* 2013). However, it is believed that this issue is not essential, and alternative assumptions can be implemented with the procedures described here (Baker 2015). For the considered systems at the different limit states pertaining to 0.5, 1, 2 and 3% maximum IDR, fragility curves are plotted comparatively in Fig. 14. For maximum IDR of 0.5%, 1% and 2%, difference between the fragility curves of the SMA-Rein., COMBINED, and STEEL-Rein. models are insignificant. For limit state corresponding to the maximum IDR of 3%, the difference between the fragility curves of SMA-Rein. and STEEL-Rein. increases while the difference between the curves of the COMBINED and STEEL-Rein. is negligible. It is obvious that the global response of COMBINED model is considerably better than that of the SMA-Rein. model. For example, for an earthquake with Sa(T1,5%) equal to 1.5 g, the probability of exceeding the 3% IDR (recognized as collapse prevention in LATBSDC) for the COMBINED and STEEL-Rein. models is approximately 47%, while this quantity is almost 74% for SMA-Rein. model. The main reason for a larger probability of exceeding the 3% IDR for an assumed Sa(T1, 5%) in SMA-Rein. model is the concentration of deformation demand at the first story subjected to very strong ground motions.

5. Conclusions

The seismic behavior of a system concurrently including distinct steel reinforced RC wall, as well as another wall with super elastic SMA reinforcing at the first story and steel rebar at upper stories, is an interesting matter. In this paper, the seismic response of such a combined system iscompared to conventional steel RC concrete walls and also to the wall with SMA rebar at the first story and steel rebar at other stories. The models are designed according to the common codes. Then, nonlinear time history analysis at

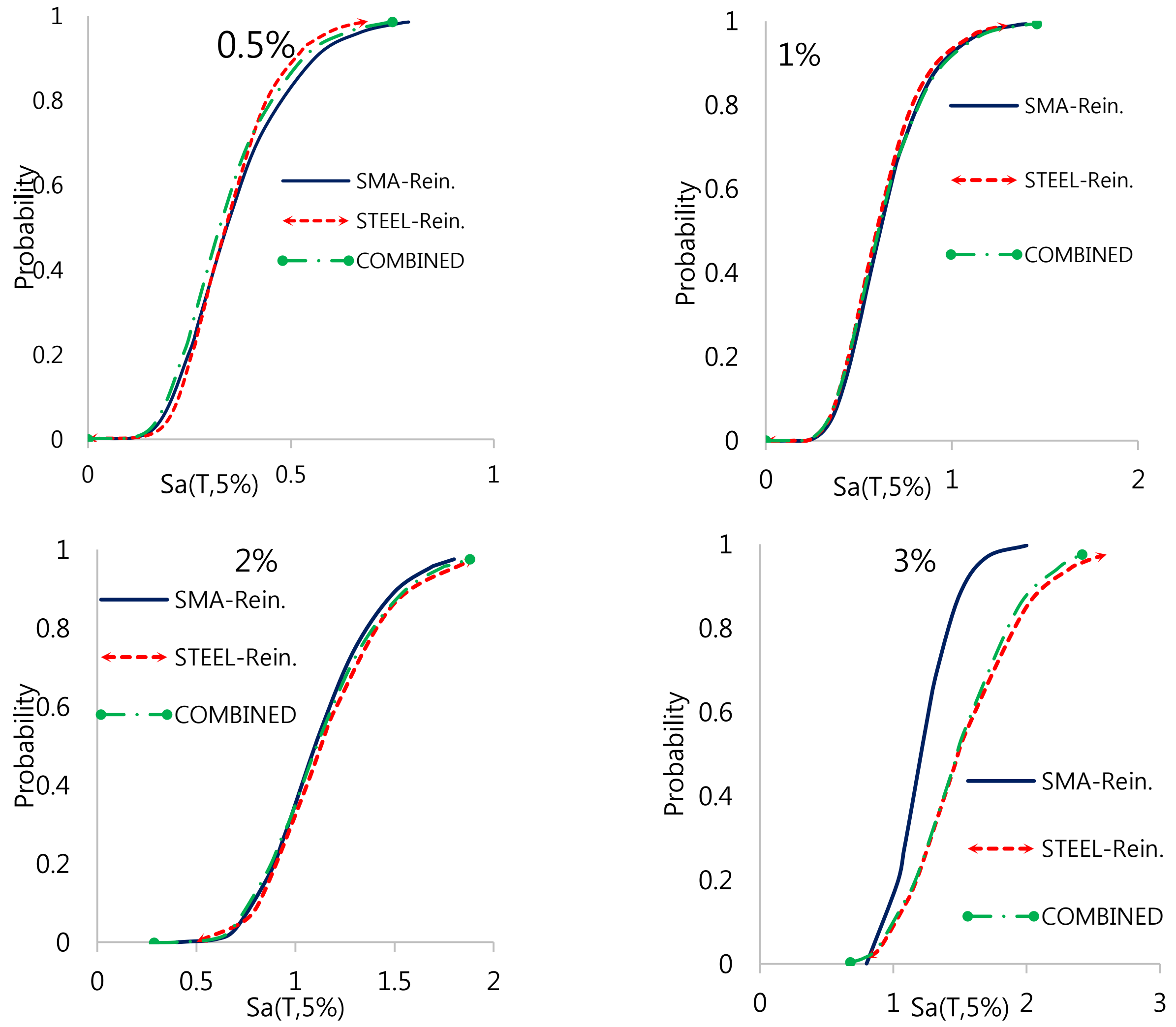

Fig. 14 Fragility curves at the different limit states pertaining to 0.5, 1, 2 and 3% maximum IDR

maximum considered and design bases earthquake level is conducted and the main responses like inter-story drift ratio and residual inter story drift ratio are investigated. Furthermore, incremental dynamic analysis is used to accomplish probabilistic seismic studies by creating fragility curves. The following results are concluded:

- Subjected to DBE level ground motion, the maximum IDR demand occurs in the STEEL-Rein. model in the last story, which is about 1.6%. The values for COMBINED and SMA-Rein. models are 1.49% and 1.4% respectively, all of which are below the permissible limit.
- The maximum residual IDR demands of the SMA-Rein., COMBINED, and STEEL-Rein. models under the influence of DBE level earthquakes are 0.05%, 0.13% and 0.18%, all of which are less than 0.5%. It is obvious that the maximum residual IDR in the SMA-Rein. model is significantly lower than its corresponding value for the other two structures. According to experts, if the amount of residual IDR in a structure under the influence of an earthquake exceeds 0.5%, the demolition of the building for renovation is almost inevitable.
- Subjected to the earthquakes at MCE level intensity, the mean maximum IDR demand in SMA-Rein. model is almost 4.6%, which is approximately twice the corresponding value in STEEL-Rein. structure. For the COMBINED model, the value is about 2.8%. LATBSDC guideline requires the average maximum IDR demand at the MCE level event to be less than 3%. Therefore, the use of SMA rebar in the first story of all walls of a structure is not recommended.
- For maximum residual IDR demand of each earthquake at the MCE level, in the model with SMA rebar in all walls of the first story (SMA-Rein. model), the average maximum IDR demand is about 0.25%. For the conventional RC wall, this quantity is about 1.27%, whereas for the COMBINED model, where only half of the walls at the first story includes SMA rebar, it is about 0.51%.
- For maximum IDRs of 0.5%, 1% and 2%, the differences between fragility curves of SMA-Rein., COMBINED, and STEEL-Rein. models are insignificant.

For the limit state corresponding to maximum IDR of 3%, the difference between fragility curves of SMA-Rein. and STEEL-Rein. increases, and the difference between the curves of the COMBINED and STEEL-Rein. is negligible. The global response of COMBINED model is considerably better than that of the SMA-Rein. model. For example, for an earthquake with Sa(T1, 5%) of 1.5 g, the probability of exceeding the 3% IDR (recognized as collapse prevention in LATBSDC) for COMBINED and STEEL-Rein. models is approximately 47%, while this quantity for SMA-Rein. model is almost 74%. Generally, the fragility curves show that using SMA rebar at the base of all walls causes a larger probability of exceeding 3% inter-story drift limit state, in comparison with a COMBINED model.

• Static push over analysis demonstrated that the strength of the COMBINED model is almost 0.35% larger than that of the two other models, and its general post-yielding stiffness is also approximately twice the corresponding stiffness of the two other models.

References

ACI 318-14, (2014), "Building code requirements for structural concrete and commentary", ACI Committee 318, Farmington Hills.

Alam, M.S., Nehdi, M. and Youssef, M.A. (2008), "Seismic performance of concrete frame structures reinforced with superelastic shape memory alloys", *Smart Struct. Syst.*, **5**(5), 565-585. http://dx.doi.org/10.12989/sss.2009.5.5.565.

American Concrete Institute (ACI). (2013), "Guide for testing reinforced concrete structural elements under slowly applied simulated seismic loads" ACI committee 374. ACI 374.2R-13. Michigan, United States.

Auricchio, F. and Sacco, E. (1997), "A superelastic shape-memory-alloy beam", *J. Intel. Mat. Str.*, **8**(6), 489-501. https://doi.org/10.1177/1045389X9700800602.

Applied Technology Council, (2010), "ATC-72: Modeling and Acceptance Criteria for Seismic Design and Analysis of Tall Buildings", ATC, Redwood City, CA.

ASCE/SEI 7-2010 (2010), "Minimum design loads for buildings and other structures", American Society of Civil Engineers. Reston, VA.

ASCE/SEI 41-13, (2014), "Seismic rehabilitation of existing buildings", American Society of Civil Engineers, Reston, VA.

Abdulridha, A., Palermo, D., Foo, S. and Vecchio, F.J. (2013), "Behavior and modeling of superelastic shape memory alloy reinforced concrete beams", *Eng. Struct.*, **49**, 893-904. https://doi.org/10.1016/j.engstruct.2012.12.041.

Abdulridha A, Palermo D. (2017), "Behaviour and modelling of hybrid SMA-steel reinforced concrete slender shear wall", Eng Struct, 147, 77–89. http://dx.doi.org/10. 1016/j.engstruct.

Alam, M.S., Nehdi, M. and Youssef, M.A. (2009), "Seismic performance of concrete frame structures reinforced with superelastic shape memory alloys", *Smart Struct. Syst.*, **5**(5), 565-585. http://dx.doi.org/10.12989/sss.2009.5.5.565.

Baker, J.W. (2015), "Efficient analytical fragility function fitting using dynamic structural analysis", *Earthq. Spectra*, **31**(1), 579-599. https://doi.org/10.1193/021113EQS025M.

Bradley, B.A. (2013), "Practice-oriented estimation of the seismic demand hazard using ground motions at few intensity levels", *Earthq. Eng. Struct. D.*, **42**(14), 2167-2185. https://doi.org/10.1002/eqe.2319.

Building Seismic Safety Council (BSSC). (2003), NEHRP Recommended Provisions for Seismic Regulations for New Buildings and Other Structures: FEMA 450; BSSC: Washington, DC, USA.

Beiraghi, H. and Siahpolo, N. (2016), "Seismic assessment of RC core-wall building capable of three plastic hinges with outrigger", *Struct. Des. Tall Spec. Build.*, **26**(2):e1306. https://doi.org/10.1002/tal.1306.

Beiraghi, H, (2017), "Earthquake effects on the energy demand of tall reinforced concrete walls with buckling-restrained brace outriggers", *Struct. Eng. Mech.*. **63**(4), 521-536. https://doi.org/10.12989/sem.2017.63.4.521.

Beiraghi H, (2018a), "Energy dissipation of reinforced concrete wall combined with buckling-restrained braces subjected to near- and far-fault earthquakes", *Iran J Sci Technol Trans Civ Eng.*, **42**(4), 345-359

Beiraghi, H. (2018b), "Energy demands in reinforced concrete wall piers coupled by buckling restrained braces subjected to near-fault earthquake", *Steel Compos. Struct.*, **27**(6), 703-716. https://doi.org/10.12989/scs.2018.27.6.703.

Beiraghi, H, (2018c), "Reinforced concrete core-walls connected by a bridge with buckling restrained braces subjected to seismic loads", *Earthq. Struct.*, **15**(2), 203-214. https://doi.org/10.12989/eas.2018.15.2.203.

Beiraghi, H, (2018d), "Near-fault ground motion effects on the responses of tall reinforced concrete walls with buckling-restrained brace outriggers", *Scientia Iranica A*, **25**(4), 1987-1999. DOI:10.24200/sci.2017.4205.

CSA Standard A23.3-04, (2005), Design of concrete structures. Canadian Standard Association: Rexdale, Canada, 214 pp.

Chancellor, N.B., Eatherton, M.R., Roke, D.A. and Akbaş, T. (2014), "Self-centering seismic lateral force resisting systems: high performance structures for the city of tomorrow", *Buildings*, **4**(3), 520-548. http://dx.doi.org/10.3390/buildings4030520.

Cruz Noguez, C.A. and Saiidi, M.S. (2013), "Performance of advanced materials during earthquake loading tests of a bridge system", *J Struct Eng.*, **139**(1), 144-154. http://dx.doi.org/10.1061/(ASCE)ST.1943-541X.0000611.

Cortés-Puentes, W.L. and Palermo, D. (2017), "SMA tension brace for retrofitting concrete shear walls", *Eng Struct*, **140**, 177-188. http://dx.doi.org/10.1016/j.engstruct.2017.02.045.

Cortés-Puentes, W.L. and Palermo D, (2018), "Seismic retrofit of concrete shear walls with SMA tension braces", *J. Struct. Eng.*, **144**(2), 04017200. https://doi.org/10.1061/(ASCE)ST.1943-541X.0001936.

CEN EC8, (2004), Design of Structures for Earthquake Resistance. European Committee for Standardization: Brussels, Belgium.

Dhakal, R.P., Mander, J.B. and Mashiko, N. (2006), "Identification of critical ground motions for seismic performance assessment of structures", *Earthq. Eng. Struct. D.*, **35**(8), 989-1008.

Elwood, K.J. (2013), "Performance of concrete buildings in the 22 February 2011 Christchurch earthquake and implications for Canadian codes", *Can. J. Civ. Eng.*, **40**(8), 759-776. http://dx.doi.org/10.1139/cjce-2011-0564.

Eberhard, M.O. and Sozen, M.A. (1993), "Member behavior-based method to determine design shear in earthquake-resistant walls", *J. Struct. Eng.*, **119**(2), 619-640. https://doi.org/10.1061/(ASCE)0733-9445(1993)119:2(619).

ETABS, Version 13.1.1. (2013), Computers and Structures. Inc.: Berkeley, California, USA

Eguchi, R.T.; Goltz, J.D.; Taylor, C.E.; Chang, S.E., Flores, P.J.; Johnson, L.A. and Blais, N.C. (1998), "Direct economic losses in the Northridge earthquake: A three-year post-event perspective", *Earthq. Spectra*, **14**(2), 245-264. https://doi.org/10.1193/1.1585998.

Eads, L., Miranda, E., Krawinkler, H. and Lignos, D.G., (2013), "An efficient method for estimating the collapse risk of structures in seismic regions", *Earthq. Eng. Struct. D.*, **42**(1), 25-41. https://doi.org/10.1002/eqe.2191.

FEMA P695, (2009), Quantification of Building Seismic Performance Factors (ATC-63 Project). Federal Emergency Management Agency, Washington D.C.

FEMA P-58. (2012), Seismic Performance Assessment of Buildings, Volume 1 - Methodology. Federal Emergency Management Agency: Washington D.C.

Federal Emergency Management Agency (FEMA). (2000), Prestandard and commentary for the seismic rehabilitation of buildings. FEMA 356. Washington, D.C.

Fintel M. (1995), "Performance of buildings with shear walls in earthquakes of the last thirty years", *PCI J*., **40**(3), 62-80.

Ghassemieh, M., Bahaari, M.R., Ghodratian, S.M. and Nojoumi, S.A. (2012), "Improvement of concrete shear wall structures by smart materials", *Open J. Civil Eng*., **2**(3), 87-95.

Ghorbanirenani, I., Tremblay, R., Léger, P. and Leclerc, M. (2012), "Shake table testing of slender rc shear walls subjected to eastern north america seismic ground motions", *J. Struct. Eng*., **138**(12), 1515-1529. https://doi.org/10.1061/(ASCE)ST.1943-541X.0000581.

Ghosh, S.K. (1995), "Observations on the performance of structures in the kobe earthquake of January 17, 1995", *PCI J*., **40**(2), 14-22.

Ibarra, L.F. and Krawinkler, H. (2005), Global Collapse of Frame Structures under Seismic Excitations, John A. Blume Earthquake Engineering Center, Stanford, CA, 324.

Janke, L., Czaderski, C., Motavalli, M. and Ruth, J. (2005), "Applications of shape memory alloys in civil engineering structures – overviews, limits and new ideas", *Mater. Struct*., **38**, 578-592.

Katariya, P.V., Panda, S.K., Hirwani, C.K., Mehar, K. and Thakare, O. (2017), "Enhancement of thermal buckling strength of laminated sandwich composite panel structure embedded with shape memory alloy fibre", *Smart Struct. Syst*., **20**(5), 595-605. https://doi.org/10.12989/sss.2017.20.5.595.

Kruep, S.J. (2007), Using incremental dynamic analysis to visualize the effects of viscous fluid dampers on steel moment frame drift. Master's Thesis. Virginia Polytechnic Institute and State University, Blacksburg, VA.

Hamdaoui, K., Benadla, Z., Chitaoui, H. and Benallal, M.E. (2019), "Dynamic behavior of a seven century historical monument reinforced by shape memory alloy wires", *Smart Struct. Syst*., **23**(4), 337-345. https://doi.org/10.12989/sss.2019.23.4.337.

LATBSDC, (2011), "An Alternative Procedure For Seismic Analysis and Design of Tall Buildings Located in the Los Angeles Region", Los Angeles Tall Buildings Structural Design Council.

Luu, H., Ghorbanirenani, I., Léger, P. and Tremblay, R. (2013), "Numerical modeling of slender reinforced concrete shear wall shaking table tests under high-frequency ground motions", *J. Earthq. Eng*., **17**(4), 517-542. https://doi.org/10.1080/13632469.2013.767759.

McCormick, J., Aburano, H., Ikenaga, M. and Nakashima, M. (2008), "Permissible residual deformation level for building structures considering both safety and human elements", *Proceedings of the 14th World Conference on Earthquake Engineering*, Beijing, China. Paper ID 05-06-0071.

Mander, J.B., Priestley, M.J.N. and Park, R. (1988), "Theoretical stress-strain model for confined concrete", *J. Struct. Eng. – ASCE*, **114**(8), 1804-1826. https://doi.org/10.1061/(ASCE)0733-9445(1988)114:8(1804).

McCormick, J., Tyber, J., DesRoches, R., Gall, K. and Maier, H.J. (2007), "Structural engineering with NiTi. II: mechanical behavior and scaling", *J. Eng. Mech*., **133**(9), 1019-1029. https://doi.org/10.1061/(ASCE)0733-9399(2007)133:9(1019).

Menegotto, M. and Pinto, P.E. (1973), "Method of analysis for cyclically loaded R.C. plane frames including changes in geometry and non-elastic behaviour of elements under combined normal force and bending", Symposium on the Resistance and Ultimate Deformability of Structures Acted on by Well Defined Repeated Loads, International Association for Bridge and Structural Engineering, Zurich, Switzerland, 15-22.

Madas P. (1993), "Advanced modelling of composite frames subjected to earthquake loading", PhD Thesis, Imperial College, University of London, London, UK.

Madas, P. (1993), "Advanced Modelling of Composite Frames Subjected to Earthquake Loading," PhD Thesis, Imperial College, University of London, London, UK.

Martínez-Rueda, J.E. and Elnashai, A.S. (1997), "Confined concrete model under cyclic load", *Mater. Struct*., **30**(3), 139-147.

Nehdi, M., Alam, M.S. and Youssef, M.A. (2011), "Seismic behaviour of repaired superelastic shape memory alloy reinforced concrete beam-column joint", *Smart Struct. Syst*., **7**(5), 329-348. http://dx.doi.org/10.12989/sss.2011.7.5.329.

National Institute of Building Sciences. (2004), Direct physical damage – general building stock, HAZUS-MH Technical manual, chapter5. Federal Emergency Management Agency: Washington, D.C.

Nakashoji, B. and Saiidi, M.S. (2014), "Seismic performance of square nickel-titanium reinforced ecc columns with headed couplers. Reno, NV, USA: Center for Civil Engineering Earthquake Research, University of Nevada.

Nehdi, M., Alam, M.S. and Youssef, M.A. (2010), "Development of corrosion-free concrete beam–column joint with adequate seismic energy dissipation", *Eng. Struct*., **32**(9), 2518-228. http://dx.doi.org/10.1016/j.engstruct.2010.04.020.

NZS 3101, (2006), New Zealand Standard, Part 1—The Design of Concrete Structures. Standards New Zealand, Wellington: New Zealand.

Orakcal, K. and Wallace, J.W. (2006), "Flexural modeling of reinforced concrete walls-experimental verification", *ACI Struct. J*., **103**(2), 196-206.

Porter, K., Kennedy, R. and Bachman, R. (2007), "Creating fragility functions for performance based earthquake engineering", *Earthq. Spectra*, **23**(2), 471-489. https://doi.org/10.1193/1.2720892.

Priestley, M.J.N., Calvi, G.M. and Kowalsky, M.J. (2007), Displacement-Based Seismic Design of Structures, IUSS Press: Pavia, Italy, ISBN: 88-6198-000-6.

Paulay, T. and Priestley, M.J.N. (1992), Seismic design of reinforced concrete and masonry buildings. Wiley: Hoboken, NJ.

Panneton, M., Léger, P. and Tremblay, R. (2006), "Inelastic analysis of a reinforced concrete shear wall building according to the National Building Code of Canada 2005", *Can. J. Civil Eng*., **33**, 854-871. https://doi.org/10.1139/l06-026.

Rutenberg, A. and Nsieri, E. (2006), "The seismic shear demand in ductile cantilever wall systems and the EC8 provisions", *Bull. Earthq. Eng*., **4**, 1-21.

Sadraddin, H.L., Shao, X. and Hu, Y. (2016), "Fragility assessment of high-rise reinforced concrete buildings considering the effects of shear wall contributions", *Struct. Des. Tall Spec. Build*., DOI: 10.1002/tal.1299.

Song, G., Ma, N. and Li, H.N. (2006), "Applications of shape memory alloys in civil structures", *Eng. Struct.*, **128**, 1266-1274.

Saatcioglu, M., Palermo, D., Ghobarah, A., Mitchell, D., Simpson, R., Adebar, P., et al. (2013), "Performance of reinforced concrete buildings during the 27 February 2010 Maule (Chile) earthquake", *Can. J. Civ. Eng*., **40**(8), 693-710.

http://dx.doi.org/10.1139/cjce-2012-0243.
Seismosoft (2018), SeismoStruct: A Computer Program for Static and Dynamic Nonlinear Analysis of Framed Structures, Version 6, http://www.seismosoft.com.
Saiidi, M.S. and Wang, H.Y. (2006), “Exploratory study of seismic response of concrete columns with shape memory alloys reinforcement”, *ACI Struct. J*., **103**(3), 436-443.
Saiidi, M.S., O’Brien, M,, Sadrossadat-Zadeh, M. (2009), “Cyclic response of concrete bridge columns using superelastic Nitinol and bendable concrete”, *ACI Struct. J*., **106**(1), 69-77.
Tremblay, R., Lacerte, M. and Christopoulos, C. (2008), “Seismic response of multistory buildings with self-centering energy dissipative steel braces”, *J. Struct. Eng*., **134**(1), 108-120. http://dx.doi.org/10.1061/(ASCE)0733-9445(2008) 134:1(108).
Vamvatsikos, D. and Cornell, CA. (2002), Seismic performance, capacity and reliability of structures as seen through incremental dynamic analysis. Report No. 151. John A. Blume Earthquake Engineering Research Center, Department of Civil and Environmental Engineering, Stanford University, Stanford, California.
Vamvatsikos, D. and Fragiadakis, M. (2010), “Incremental dynamic analysis for estimating seismic performance sensitivity and uncertainty”, *Earthq. Eng. Struct. D*., **39**(2), 141-163. https://doi.org/10.1002/eqe.935.
Wallace, J.W. (2012), “Behavior, design, and modeling of structural walls and coupling beams — Lessons from recent laboratory tests and earthquakes”, *Int. J. Concr. Struct. Mater*., **6**(1), 3-18. http://dx.doi.org/10.1007/s40069-012-0001-4.
Youssef, M.A., Alam, M.S. and Nehdi, M. (2008), “Experimental investigation on the seismic behavior of beam-column joints reinforced with superelastic shape memory alloys”, *J. Earthq. Eng*,, **12**(7), 1205-1222. http://dx.doi.org/10.1080/13632460802003082.
Youssef, M.A. and Elfeki, M.A. (2012), “Seismic performance of concrete frames reinforced with superelastic shape memory alloys”, *Smart Struct. Syst*., **9**(4), 313-333. http://dx.doi.org/10.12989/sss.2012.9.4.313

CC